

# ON-ORBIT GEOMETRIC CALIBRATION OF THE ORBVIEW-3 HIGH RESOLUTION IMAGING SATELLITE

David Mulawa, Ph.D

ORBIMAGE, 1835 Lackland Hill Parkway, St. Louis, MO 63146, USA – mulawa.david@orbimage.com

**KEY WORDS:** calibration, geometric, satellite, camera, accuracy

## ABSTRACT:

Current high resolution satellite design includes several sensor types such as: GPS receivers, star trackers, rate gyros and cameras. In order to produce high quality metric imagery, the on-orbit data from all of these sensors need to be combined in a calibration process to produce the geometric model parameters of the sensor system. The calibration process is also used to determine an on-orbit stochastic model for the sensors and the estimated calibration parameters.

The OrbView-3 (OV-3) on-orbit geometric calibration is based on the mathematical modelling and estimation of calibration parameters incorporated into a rigorous and flexible self-calibration triangulation, Kalman filter software suite and orbit determination software. The principal components of the geometric model are: orbit determination, attitude determination and camera model. The satellite orbit determination is based on the GIPSY-OASIS software from Jet Propulsion Lab (JPL). The calibration of the attitude determination system uses an Alignment Kalman Filter to estimate the alignment angles and gyro scale factor calibration parameters associated with the star trackers and rate gyros. Medium scale aerial imagery is used to form the basis of a geometric camera calibration range. To reduce the collection time and improve the quality of the camera calibration solution, the calibration range imagery is combined with image correlation software techniques to automatically acquire tie points with the satellite imagery and to allow the assembly of an extremely dense collection of ground control points

The operational geolocation accuracy performance of the OV-3 satellite is represented by the observed geolocation accuracy at several test sites.

## 1. INTRODUCTION

Imaging satellites are subjected to several factors that may cause the values of the geometric calibration parameters to vary between the time of ground calibration and on-orbit operation. Some of these are: launch shock; loss of moisture due to vacuum; and gravity release. The ground calibration process is used to obtain the best a priori estimates of the on-orbit values of the calibration parameters. Generally, the satellite builder can perform mechanical analyses to estimate the range in which the critical calibration parameters are expected to change between ground calibration and on-orbit use.

The geometric calibration plan for the OrbView-3 (OV-3) satellite calls for an initial geometric calibration during the satellite commissioning phase and periodic geometric calibrations thereafter. There is a significant effort associated with the initial calibration. However, the accumulated magnitude of effort involved with the periodic geometric calibrations over the life of the satellite will surpass the one time initial effort. It is important that the on-orbit geometric calibration method be able to take advantage of autonomous methods as much as possible in order to drive down the effort and time required to perform the periodic geometric calibrations.

## 2. GEOMETRIC CALIBRATION RANGE

The OV-3 Geometric Calibration Range is a metric standard that the OrbView-3 satellite data was compared against during geometric camera calibration. In order to provide the best georeferencing capability from the satellite systems, it

is necessary that the calibration range have both good absolute and relative accuracies.

Cost should also be considered. The calibration range should be cost effective to create, use and maintain. Two types of ranges can be considered: ground surveyed photo identifiable points and controlled aerial photography. The use of controlled aerial photography offers many advantages. For example, the calibration range is the set of aerial photographs and support data. As many ground control points as are needed can be generated from the set of aerial photographs. Powerful image correlation methods can be used to help reduce the cost and time needed to measure the control points in the aerial and satellite imagery. In terms of maintenance, if some of the photographs become unusable due to changes in the ground texture, such as new construction, additional aerial photography can be flown and triangulated into the block.

The OV-3 Geometric Calibration Range covers an area of 50km in the north-south direction and 50km in the east-west direction. The aerial photographs were acquired with a standard frame mapping camera at a scale of 1:25,000. All the points in the interior of the calibration range appear on a minimum of 4 photographs and some points fall on 9 photographs. This redundancy leads to reliability suitable for a geometric calibration range.

Ground control of the aerial photographs was provided through targeted GPS survey points. The exposure stations of the aerial photographs were acquired with differential GPS in order to: increase redundancy; stiffen the block; and to allow an improved self-calibration of the aerial mapping camera.

The aerial photographs were scanned with a pixel size of 14 microns. At this photo scale, the nominal pixel ground sample distance is 35 cm. The complete set of image scans has a storage requirement of 150GB.

### 3. CALIBRATION SOFTWARE

The main software components that were used to perform the geometric calibration of the OrbView-3 satellite are: Alignment Kalman Filter, orbit determination, image correlator, and multi-sensor triangulation. Each of these is described in sections below. The image correlator and the triangulation software were also used to build the Geometric Calibration Range.

#### 3.1 Alignment Kalman Filter

The exterior attitude orientation of the OV-3 satellite is determined by using star trackers and gyroscopes. The star trackers provide an absolute attitude reference at a discrete sampling rate. The gyros provide relative attitude changes at a fast sampling rate. The data from the star trackers and gyros is blended in a Kalman filter to estimate the platform attitude in an absolute attitude reference frame at a high sample rate with good relative attitude changes.

In order to obtain accurate platform attitude estimates the geometric calibration process needs to determine the alignment angles between the star trackers and the gyros coordinate axes. This is accomplished by carrying these alignment angles as parameters to be estimated in an algorithm called the Alignment Kalman Filter. Additional parameters estimated by the Alignment Kalman Filter include: gyro bias and scale factors. This filter can be thought of as a self-calibration process. For the alignment angles to be observable (estimable), the spacecraft has to maneuver through a sufficient volume of 3D attitude space and at different angular rates. The alignment angles between the gyro and camera axes are determined in the triangulation model.

#### 3.2 Orbit Determination

The orbit determination software is Gipsy-Oasis and is maintained by JPL (Jet Propulsion Laboratory). Gipsy-Oasis contains sophisticated orbital models that include components such as: gravity model, drag model, stochastic force model, and a GPS receiver model. Precision orbit determination uses the Rapid Product from the IGS (International GPS Service) for post-processed GPS ephemerides.

#### 3.3 Image Correlator

A flexible and efficient image correlator is key to the cost effective use of controlled aerial photography for control point generation. Since the image correlator needs to locate common image points in both the aerial and satellite imagery, it must work well with non-homogenous image sets. The differences between the aerial and satellite imagery can be caused by temporal effects, such as fields with different crops, or by image scale and rotation. The image correlator reduces scale and rotation differences by rectifying both image sources to the same scale and orientation. The rectification is performed on the fly. The image correlation is performed on the rectified imagery and the image coordinates of the match points are transformed back into the coordinate systems of the original images.

#### 3.4 Multi-Sensor Triangulation

Triangulation software is used to estimate the camera calibration parameters. This software needs to be rigorous, flexible and robust. The design of the triangulation software follows an object oriented approach that includes a framework structure, utilities and a Developers Took Kit (DTK). The DTK is the used to rapidly bring in new sensor models. The formal division between framework and sensor factory allows the sensor developer to focus in on the sensor I/O and math model in the DTK and the framework contains the memory management and the least squares adjustment engine [Mulawa 2000]. The OV-3 geometric camera calibration model contains parameters to model the interior orientation, distortion and camera alignment to platform.

### 4. ON-ORBIT GEOMETRIC CALIBRATION OF OV-3

The on-orbit geometric calibration of a system having as many sensors as a high resolution imaging satellite takes place over a period of time and is accomplished by the achievement of milestones events. It is this method that is used in this paper to describe the geometric calibration process. The calibration process has many experts involved in tuning and calibration of the sensor components that they are responsible for. While a substantial amount of work is done in parallel by the geometric calibration team members on sensor components, there is also a sequential approach to bringing the system into calibration. For example: camera focus, orbit determination and the attitude determination systems must be calibrated prior to completion of the camera calibration. The camera calibration is the last step in the on-orbit calibration of the satellite.

#### 4.1 Milestone Events

OV-3 Launched	2003 July 26
First Image	2003 July 27
Initial Calibration of the Attitude Determination System	2003 July 27
Coarse Boresight Adjustment	2003 Aug 22
Final Camera Focus Adjustment	2003 Sep 05
Orbit determination model tuned and verified	2003 Sep 17
Coarse geometric camera calibration	2003 Sep 17
Refined calibration of the attitude determination system	2003 Oct 03
Initial geometric camera calibration	2003 Nov 04

Table 1: OV-3 Geometric Calibration Milestone Events

#### 4.2 OV-3 Launched: 2003 June 26

The launch vehicle performed well and placed OV-3 into its nominal orbit. The satellite beacon was heard on the first pass over the northern terminal. Command and control of the satellite was established. During the next month, the camera door remained closed while the satellite was out-gassed and was raised to its final orbit. A series of tests were performed to ensure the safe operation of the satellite.

### 4.3 First Image: 2003 July 26

The first image was collected over the east coast of the United States. This first image began a chain of events related to the on-orbit tuning and calibration of the camera. Some of the events include: image quality assessment, camera focusing, radiometric calibration and geometric calibration.

### 4.4 Initial Calibration of the Attitude Determination System: 2003 July 27

The initial calibration of the attitude determination system represented the first major milestone in the on-orbit geometric calibration of the satellite. This step determined the alignments between the star trackers and the gyros. Also determined were the on-orbit performance characteristics of the star trackers and the gyros. The truth data used in this calibration step was the reference stars in the star tracker's catalog.

Much of this calibration step was accomplished while the camera door was closed. This calibration also included a special maneuver that was designed to move the vehicle in an optimum way to provide reliable alignment estimates.

### 4.5 Coarse Boresight Adjustment: 2003 Aug 22

This step was used to improve the boresight alignment of the camera. Imagery from the geometric calibration range was used to establish a boresight error of less than 100 meters.

### 4.6 Final Camera Focus Adjustment: 2003 Sep 05

The initial days of operating the camera were filled with many activities, including achieving the best focus of the camera. There is a flat focus mirror inside the camera that can be moved by very small amounts to improve the focus. The mirror was moved several times until the best focus was achieved based on a metric assessment that involved the examination of edge sharpness in the imagery [Kohm and Tira 2004]. The movement of the mirror causes changes in the focal length and optical distortion of the camera, therefore only imagery collected after the focus had been set could be used in the initial geometric calibration of the camera.

### 4.7 Orbit Determination Model Tuned and Verified: 2003 Sep 17

JPL performed the tuning and verification of the orbit determination model [Kuang 2004]. The postfit range residual after tuning was less than 1 meter (RMS). The formal sigma of orbital positioning error is the propagated a posteriori error estimate and was less than 1 meter. Another test is also performed in computing two time periods with an overlap in time. This showed differences that were less than 1 meter in 3D.

The following measurement and dynamic models are used in OV3 orbit determination:

- 27 hour orbit arc (nominal)
- BENT ionosphere model, estimating one scale factor per arc
- 70x70 gravity model from GRACE data
- Satellite model of one solar panel with one cylinder for drag and solar pressure

- Satellite attitude determined by the quaternion measurement
- Atmospheric drag, estimating one scale factor per arc
- Solar radiation pressure, fixed
- Empirical once-per-revolution cross-track and along-track forces
- Stochastic radial, cross-track and along-track forces
- White noise receiver clock bias estimated at every 5 minute
- Random-walk clock offset between receiver antennas estimated at every 20 minute

Date	P1 Data Residual RMS (m)	Number of Points	Number of Outliers
03JUL06	0.96	2300	22
03JUL07	0.98	1837	21
03JUL08	0.98	2065	243
03JUL19	0.84	1832	13
03JUL20	0.86	2149	20
03JUL21	0.84	1953	23

Table 2: RMS of Range Residuals from Orbit Determination

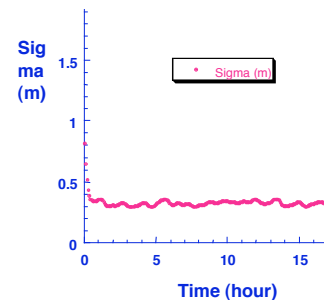


Figure 3: 3D Formal Sigma from Orbit Determination

### 4.8 Coarse Geometric Calibration of the Camera: 2003 Sep 17

A coarse geometric calibration of the camera was performed using the imagery from the first pass over the geometric calibration range after the focus had been set. This coarse calibration estimated first order effects such as camera alignment, focal length and smile distortion. Other effects, such as scale distortion were not estimated until more image data was available and the calibration had been refined for the attitude determination system.

### 4.9 Refined Calibration of the Attitude Determination System: 2003 Oct 03

Additional data is brought into the calibration process for the attitude determination system to improve the reliability of the calibration parameters. The estimated accuracy of the alignment between the star tracker and gyro axes is 0.5 arcsecond (1 sigma).

### 4.10 Initial Geometric Calibration of the Camera: 2003 Nov 04

The initial geometric calibration of the camera used data from 13 panchromatic and 2 multispectral images collected during the period from: 2003 Sep 10 to 2003 Oct 27. Each of the multispectral bands represented a separate image for calibration purposes. Thus, 13+8=21 images were used in the initial geometric camera calibration. The imagery was

collected in a variety of scan directions that included: north-south, south-north, east-west and west-east scan directions. The footprints of the imagery used in the initial geometric camera calibration of OV-3 can be seen in Figure 4 shown below.

All of the image measurements were collected by auto correlation methods. There were a total of 3,875 ground control points from the geometric calibration range. A total of 33,093 image rays were observed on the satellite images. This means that each ground control point was observed on an average of 8.5 images. Some of the ground control points at the center of the geometric calibration range were observed on all of the images. Figure 4 shows the location of the ground control points generated from the geometric calibration range shown as blue triangles.

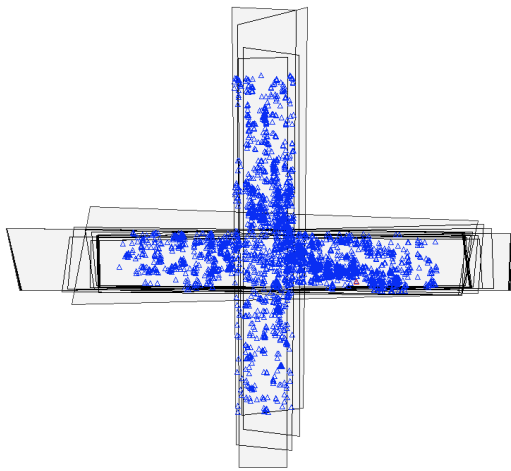


Figure 4: Imagery Footprints and Control Points Used in the Initial Geometric Camera Calibration of OV-3

An advantage to using controlled aerial photographs is that a large number of control points can be used for the characterization and calibration of the camera. Figures 5-8 show the image residuals from the panchromatic arrays. Each dot in the graph represents an observation of a ground control point. It is clear that the ground control densely covers the entire arrays.

To show apparent distortions at the focal plane, an adjustment solving for only the focal length and camera alignment parameters was performed. The resulting image residuals show the remaining optical and focal plane distortions. The distortion is divided into two separate directions: line and sample residuals. The distortion in the line direction is sometimes called the camera smile distortion because of the characteristic shape. This distortion is primarily due to radial distortion of the optical system and is estimated in the design process of the camera. The predicted smile distortion from the camera design process agrees with the on-orbit observed distortion.

The distortion in the sample direction is parallel to the direction of the arrays. Distortions in this direction can be thought of as scale distortions along the arrays. The major contributor to this distortion is due to radial distortion of the telescope and is estimated in the camera design process. The predicted scale distortion from the camera design process agreed with the on-orbit observed distortion.

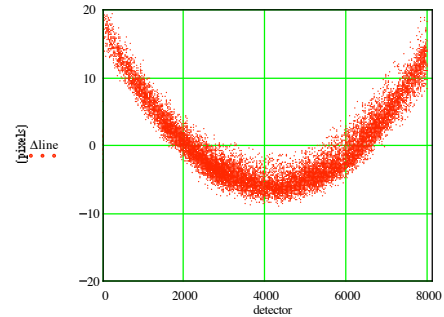


Figure 5: Image Residuals in Line Direction Showing Smile Distortion Before Camera Calibration

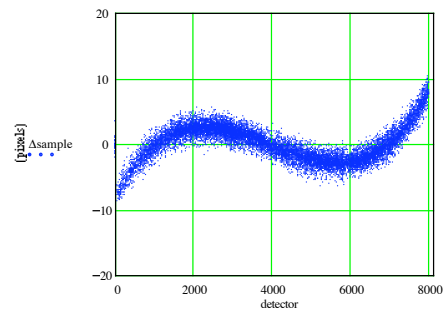


Figure 6: Image Residuals in Sample Direction Showing Scale Distortion Before Camera Calibration

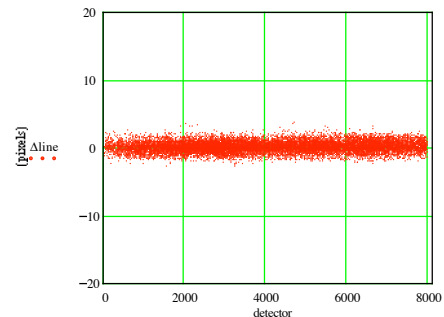


Figure 7: Image Residuals in Line Direction After Camera Calibration

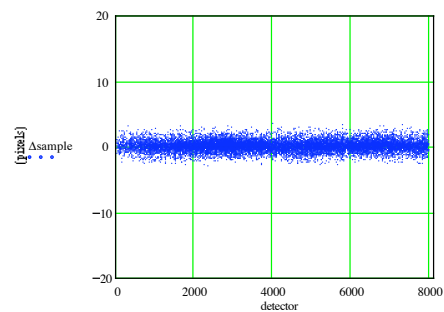


Figure 8: Image Residuals in Sample Direction After Camera Calibration

Figures 5 and 6 show the observed distortion before the initial geometric camera calibration. Figures 7 and 8 show the image residuals after the initial calibration all of the systematic distortion has been modelled in the calibration.

The standard error of the control point movement in the adjustment was (0.4, 0.4, 0.1) meters (1 sigma). The a posteriori standard error of the focal length estimate was 48 micrometers (1 sigma). This equates to less than 0.1 pixels at the end of the linear array. The a posteriori standard error estimate for the roll and pitch camera alignments were 0.5 arc seconds.

The completion of the camera calibration is the last step in the initial geometric calibration of OV-3. Various test site data used to validate the calibration is shown in the next section.

### 5. GEOLOCATION ACCURACY RESULTS

The validation of the calibration and the end-to-end system performance evaluation is done through a series of geolocation accuracy assessments. These assessments are evaluations of the system performance compared to exterior control data.

This section shows the results of two types of geolocation accuracy assessment of OV-3 imagery: monodrop, and stereo comparisons.

The check points used in the geolocation accuracy assessments consist of photo-identifiable ground survey points in sites around the world. The imagery was collected over a period of 5 months and demonstrates the stability of the calibration parameters.

Generally, a geolocation accuracy assessment tends to show a small diameter cluster of differences for the points from a mono image or stereo pair. However, the mean of the cluster is not usually zero and represents a bias for the image or stereo pair. These biases change from image to image and are said to be random. Random bias scatter plots are shown in the figures below.

#### 5.1 Monodrop Comparison

The monodrop comparison used imagery had not been adjusted through the inclusion of tie points or control points and represents the direct positioning capability of the system. To perform a monodrop comparison, the measured image coordinates were projected down to the elevation of the check point to determine the latitude and longitude observed by OV-3. The difference between the latitude and longitude observed by OV-3 and the check point are computed and aggregated to form test statistics such as CE. The imagery was collected in a variety of scan directions that included: north-south, south-north, east-west and west-east scan directions. In all, 72 images were used in this assessment.

The monodrop CE histogram has a median value of 9 meters and a mean value of 10 meters. The 90-th percentile of the CE histogram is 18 meters. There is a significant skew to this CE sample, which is expected when considering CE as a random variable. There seems to be some variation as to which metric to use in discussing the geolocation accuracy of the system. The median CE and the mean CE give somewhat optimistic views to the system performance and do not address the variability in performance.

The 90-th percentile of the monodrop random biases sample ranked according to radial distance from the origin is 14 meters and is shown as the blue dashed line in Figure 10.

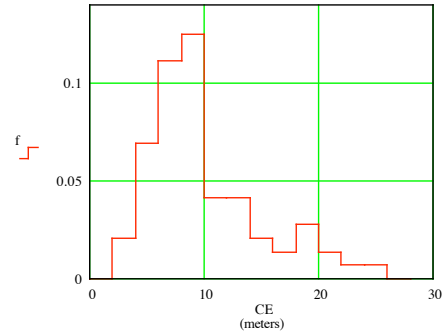


Figure 9: Monodrop Circular Error Histogram

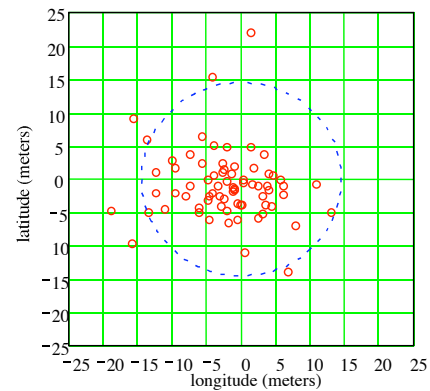


Figure 10: Monodrop Random Bias

#### 5.2 Stereo Pairs Comparison

The stereo pairs comparison also used the measured image coordinates with the post-processed ephemeris and attitude history data. A relative triangulation was performed using only tie points. The 3D coordinates of the check points were determined by space intersection within the triangulation. The differences between the latitude and longitude observed by OV-3 and the check points were determined and aggregated to form the CE test statistic. The difference in elevation observed by OV-3 and the check points was used to form the linear error (LE) test statistic.

The stereo pairs comparison test data consists of 15 stereo pairs located world wide. Due to the smaller sample size, the histogram bins were enlarged to 3 meters.

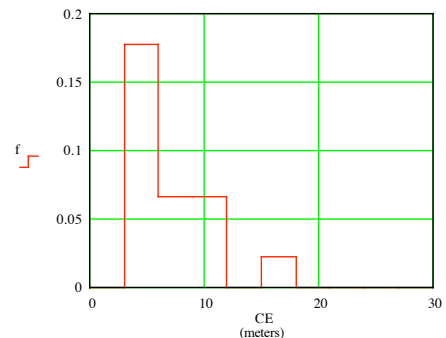


Figure 11: Stereo Pair Circular Error Histogram

The stereo pair CE histogram of the stereo pairs has a median value of 6 meters and a mean value of 7.1 meters. The 90-th percentile of the stereo pairs CE sample is 11 meters. The same skew pattern observed in the monodrop comparison is present in the stereo comparison. There is a noticeable improvement in geolocation accuracy over the unadjusted monodrop images. The act of relative triangulation helps reduce some of the effects of random error.

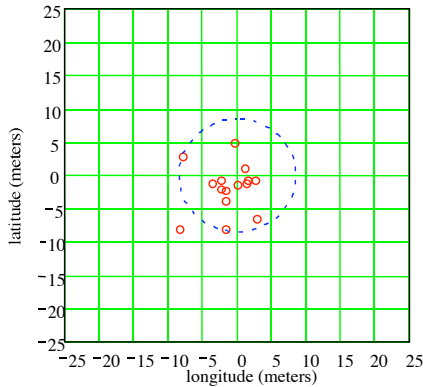


Figure 12: Stereo Pairs Random Bias

The 90-th percentile of the stereo pairs random biases sample ranked according to radial distance from the origin is 8 meters and is shown as the blue dashed line in Figure 12.

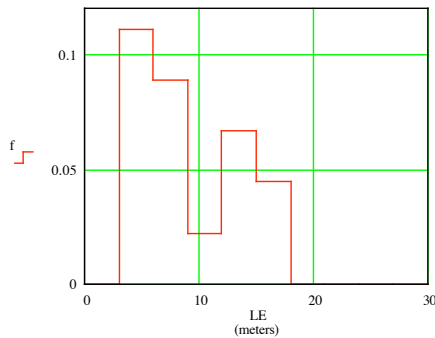


Figure 13: Stereo Pairs Linear Error Histogram

The stereo pair LE histogram of the stereo pairs has a median value of 8 meters and a mean value of 9.1 meters. The 90-th percentile of the stereo pairs LE sample is 16 meters. The same skew pattern observed in the monodrop and stereo pairs CE comparisons is present in the stereo pairs LE comparison.

## 6. DISCUSSION

Obtaining the maximum system performance for a complex system like OV-3 takes place over a period of time. As the system is exercised, improvements are made in system models, tuning and operation of the system. The largest improvements in system performance are expected to occur early in the program and later improvements are expected to be incrementally smaller. Towards the end of its life, the components may degrade and system performance can suffer. It may be difficult to predict the exact shape of the performance curve in advance. Figure 14 shows a nominal expectation of the system performance over time.

The OV-3 system performance has exceeded the level of operational maturity and additional improvements in performance are expected.

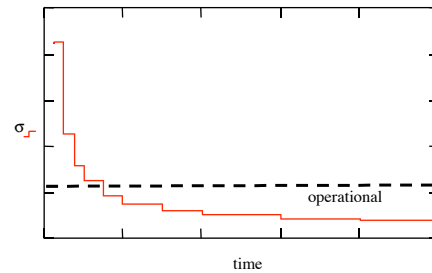


Figure 14: Expectation of System Performance Over Time

## 7. CONCLUSIONS

In the above sections the calibration software and calibration range used to perform the on-orbit geometric calibration of OV-3 have been described. The on-orbit geometric calibration of OV-3 has proceeded through a series of steps concluding with the geometric camera calibration. System level tests using comparisons to ground check points have validated the operational geolocation accuracy performance and the stability of the calibration parameters of OV-3.

## REFERENCES

- Kohm, K. and Tira, N., 2004, On-Orbit Image Quality and Radiometric Characterization of the OrbView-3 High Resolution Imaging Satellite, Accepted for publication in: *Proceedings of the ASPRS 2004 Annual Conference, May 23-28, 2004.*
- Kuang, D., 2004. Evaluation of the OV3 Orbit Accuracy. *JPL.*
- Mulawa, D., 2000. Preparations for the On-Orbit Geometric Calibration of the OrbView 3 and 4 Satellites, *The International Archives of the Photogrammetry, Remote Sensing and Spatial Information Sciences, Amsterdam, Vol. XXXIII, Part B1, Book 1, pp. 209-213.*